Fast Parallel Algorithms

for

Short–Range Molecular Dynamics

Steve Plimpton

Parallel Computational Sciences Department 1421, MS 1111

Sandia National Laboratories

Albuquerque, NM   87185-1111

(505) 845-7873

sjplimp@cs.sandia.gov

Abstract

Three parallel algorithms for classical molecular dynamics are presented. The first assigns each processor a fixed subset of atoms; the second assigns each a fixed subset of inter–atomic forces to compute; the third assigns each a fixed spatial region. The algorithms are suitable for molecular dynamics models which can be difficult to parallelize efficiently — those with short–range forces where the neighbors of each atom change rapidly. They can be implemented on any distributed–memory parallel machine which allows for message–passing of data between independently executing processors. The algorithms are tested on a standard Lennard–Jones benchmark problem for system sizes ranging from 500 to 100,000,000 atoms on several parallel supercomputers — the nCUBE 2, Intel iPSC/860 and Paragon, and Cray T3D. Comparing the results to the fastest reported vectorized Cray Y–MP and C90 algorithm shows that the current generation of parallel machines is competitive with conventional vector supercomputers even for small problems. For large problems, the spatial algorithm achieves parallel efficiencies of 90% and a 1840–node Intel Paragon performs up to 165 faster than a single Cray C90 processor. Trade–offs between the three algorithms and guidelines for adapting them to more complex molecular dynamics simulations are also discussed.

1 Introduction

Classical molecular dynamics (MD) is a commonly used computational tool for simulating the properties of liquids, solids, and molecules [1, 2]. Each of the N atoms or molecules in the simulation is treated as a point mass and Newton's equations are integrated to compute their motion. From the motion of the ensemble of atoms a variety of useful microscopic and macroscopic information can be extracted such as transport coefficients, phase diagrams, and structural or conformational properties. The physics of the model is contained in a potential energy functional for the system from which individual force equations for each atom are derived.

MD simulations are typically not memory intensive since only vectors of atom information are stored. Computationally, the simulations are "large" in two domains — the number of atoms and number of timesteps. The length scale for atomic coordinates is Angstroms; in three dimensions many thousands or millions of atoms must usually be simulated to approach even the sub–micron scale. In liquids and solids the timestep size is constrained by the demand that the vibrational motion of the atoms be accurately tracked. This limits timesteps to the femtosecond scale and so tens or hundreds of thousands of timesteps are necessary to simulate even picoseconds of "real" time. Because of these computational demands, considerable effort has been expended by researchers to optimize MD calculations for vector supercomputers [24, 30, 36, 45, 47] and even to build special–purpose hardware for performing MD simulations [4, 5]. The current state–of–the–art is such that simulating ten– to hundred–thousand atom systems for picoseconds takes hours of CPU time on machines such as the Cray Y–MP.

The fact that MD computations are inherently parallel has been extensively discussed in the literature [11, 22]. There has been considerable effort in the last few years by researchers to exploit this parallelism on various machines. The majority of the work that has included implementations of proposed algorithms has been for single–instruction/multiple–data (SIMD) parallel machines such as the CM–2 [12, 52], or for multiple–instruction/multiple–data (MIMD) parallel machines with a few dozens of processors [26, 37, 39, 46]. Recently there have been efforts to create scalable algorithms that work well on hundred– to thousand–processor MIMD machines [9, 14, 20, 41, 51]. We are convinced that the message–passing model of programming for MIMD machines is the only one that provides enough flexibility to implement all the data structure and computational enhancements that are commonly exploited in MD codes on serial and vector machines. Also, we have found that it is only the current generation of massively parallel MIMD machines with hundreds to thousands of processors that have the computational power to be competitive with the fastest vector machines for MD calculations.

In this paper we present three parallel algorithms which are appropriate for a general class of MD problems that has two salient characteristics. The first characteristic is that forces are limited in range, meaning each atom interacts only with other atoms that are geometrically nearby. Solids and liquids are often modeled this way due to electronic screening effects or simply to avoid the computational cost of including long–range Coulombic forces. For short–range MD the computational effort per timestep scales as N, the number of

atoms.

The second characteristic is that the atoms can undergo large displacements over the duration of the simulation. This could be due to diffusion in a solid or liquid or conformational changes in a biological molecule. The important feature from a computational standpoint is that each atom's neighbors change as the simulation progresses. While the algorithms we discuss could also be used for fixed–neighbor simulations (e.g. all atoms remain on lattice sites in a solid), it is a harder task to continually track the neighbors of each atom and maintain efficient $O(N)$ scaling for the overall computation on a parallel machine.

Our first goal in this effort was to develop parallel algorithms that would be competitive with the fastest methods on vector supercomputers such as the Cray. Moreover we wanted the algorithms to work well on problems with small numbers of atoms, not just for large problems where parallelism is often easier to exploit. This is because the vast majority of MD simulations are performed on systems of a few hundred to several thousand atoms where N is chosen to be as small as possible while still accurate enough to model the desired physical effects [8, 44, 38, 53]. The computational goal in these calculations is to perform each timestep as quickly as possible. This is particularly true in non–equilibrium MD where macroscopic changes in the system may take significant time to evolve, requiring millions of timesteps to model. Thus, it is often more useful to be able to perform a $100,000$ timestep simulation of a 1000 atom system fast rather than 1000 timesteps of a $100,000$ atom system, though the $O(N)$ scaling means the computational effort is the same for both cases. To this end, we consider model sizes as small as a few hundred atoms in this paper.

For very large MD problems, our second goal in this work was to develop parallel algorithms that would be scalable to larger and faster parallel machines. While the timings we present for large MD models (10^5 to 10^8 atoms) on the current generation of parallel supercomputers (hundreds to thousands of processors) are quite fast compared to vector supercomputers, they are still too slow to allow long–timescale simulations to be done routinely. However, our large–system algorithm scales optimally with respect to N and P (the number of processors) so that as parallel machines become more powerful in the next few years, algorithms similar to it will enable larger problems to be studied.

Our earlier efforts in this area [40] produced algorithms which were fast for systems with up to tens of thousands of atoms but did not scale optimally with N for larger systems. We improved on this effort to create a scalable large–system algorithm in [41]. The spatial–decomposition algorithm we present here is also unique in that it performs well on relatively small problems (only a few atoms per processor). In addition, we have added an idea due to Tamayo and Giles [51] that has improved the algorithm's performance on medium–sized problems by reducing the inter–processor communication requirements. We have also recently developed a new parallel algorithm (force–decomposition) which we present here in the context of MD simulations for the first time. It offers the advantages of both simplicity and speed for small to medium–sized problems.

In the next section, the computational aspects of MD are highlighted and efforts to speed the calculations on vector and parallel machines are briefly reviewed. In Sections 3, 4, and 5 we describe our three parallel algorithms in detail. A standard Lennard–Jones benchmark calculation is outlined in Section 6. In Section

7, implementation details and timing results for the parallel algorithms on several massively parallel MIMD machines are given and comparisons made to Cray Y–MP and C90 timings for the benchmark calculation. Discussion of the scaling properties of the algorithms is also included. Finally, in Section 8, we give guidelines for deciding which parallel algorithm is likely to be fastest for a particular short–range MD simulation.

2   Computational Aspects of Molecular Dynamics

The computational task in a MD simulation is to integrate the set of coupled differential equations (Newton's equations) given by

$$
\begin{aligned}
m_i \frac{d\vec{v}_i}{dt} &= \sum_j F_2(\vec{r}_i, \vec{r}_j) + \sum_j \sum_k F_3(\vec{r}_i, \vec{r}_j, \vec{r}_k) + \cdots \qquad (1) \\
\frac{d\vec{r}_i}{dt} &= \vec{v}_i
\end{aligned}
$$

where m_i is the mass of atom i, $\vec{r}_i$ and $\vec{v}_i$ are its position and velocity vectors, F_2 is a force function describing pairwise interactions between atoms, F_3 describes three–body interactions, and many–body interactions can be added. The force terms are derivatives of energy expressions in which the energy of atom i is typically written as a function of the positions of itself and other atoms. In practice, only one or a few terms in equation (1) are kept and F_2, F_3, etc. are constructed so as to include many–body and quantum effects. To the extent the approximations are accurate these equations give a full description of the time–evolution of the system. Thus, the great computational advantage of classical MD, as compared to *ab initio* electronic structure calculations, is that the dynamic behavior of the atomic system is described empirically without having to solve Schrodinger's equation at each timestep.

The force terms in equation (1) are typically non–linear functions of the distance r_{ij} between pairs of atoms and may be either long–range or short–range in nature. For long–range forces, such as Coulombic interactions in an ionic solid or biological system, each atom interacts with all others. Directly computing these forces scales as N^2 and is too costly for large N. Various approximate methods overcome this difficulty. They include particle–mesh algorithms [31] which scale as $f(M)N$ where M is the number of mesh points, hierarchical methods [6] which scale as $N \log(N)$, and fast–multipole methods [23] which scale as N. Recent parallel implementations of these algorithms [19, 56] have improved their range of applicability for many–body simulations, but because of their expense, long–range force models are not commonly used in classical MD simulations.

By contrast, short–range force models are used extensively in MD and is what we are concerned with in this paper. They are chosen either because electronic screening effectively limits the range of influence of the interatomic forces being modeled or simply to truncate the long–range interactions and lessen the computational load. In either case, the summations in equation (1) are restricted to atoms within some small region surrounding atom i. This is typically implemented using a cutoff distance r_c, outside of which

all interactions are ignored. The work to compute forces now scales linearly with N. Notwithstanding this savings, the vast majority of computation time spent in a short–range force MD simulation is in evaluating the force terms in equation (1). The time integration typically requires only 2-3% of the total time. To evaluate the sums efficiently requires knowing which atoms are within the cutoff distance r_c at every timestep. The key is to minimize the number of neighboring atoms that must be checked for possible interactions since calculations performed on neighbors at a distance $r > r_c$ are wasted computation. There are two basic techniques used to accomplish this on serial and vector machines; we discuss them briefly here since our parallel algorithms incorporate similar ideas.

The first idea, that of neighbor lists, was originally proposed by Verlet [55]. For each atom, a list is maintained of nearby atoms. Typically, when the list is formed, all neighboring atoms within an extended cutoff distance $r_s = r_c + \delta$ are stored. The list is used for a few timesteps to calculate all force interactions. Then it is rebuilt before any atom could have moved from a distance $r > r_s$ to $r < r_c$. Though δ is always chosen to be small relative to r_c, an optimal value depends on the parameters (e.g. temperature, diffusivity, density) of the particular simulation. The advantage of the neighbor list is that once it is built, examining it for possible interactions is much faster than checking all atoms in the system.

The second technique commonly used for speeding up MD calculations is known as the link-cell method [32]. At every timestep, all the atoms are binned into 3–D cells of side length d where $d = r_c$ or slightly larger. This reduces the task of finding neighbors of a given atom to checking in 27 bins — the bin the atom is in and the 26 surrounding ones. Since binning the atoms only requires $O(N)$ work, the extra overhead associated with it is acceptable for the savings of only having to check a local region for neighbors.

The fastest MD algorithms on serial and vector machines use a combination of neighbor lists and link–cell binning. In the combined method, atoms are only binned once every few timesteps for the purpose of forming neighbor lists. In this case atoms are binned into cells of size $d \geq r_s$. At intermediate timesteps the neighbor lists alone are used in the usual way to find neighbors within a distance r_c of each atom. This is a significant savings over a conventional link–cell method since there are far fewer atoms to check in a sphere of volume $4\pi r_s^3/3$ than in a cube of volume $27r_c^3$. Additional savings can be gained due to Newton's 3rd law by only computing a force once for each pair of atoms (rather than once for each atom in the pair). In the combined method this is done by only searching half the surrounding bins of each atom to form its neighbor list. This has the effect of storing atom j in atom i's list, but not atom i in atom j's list, thus halving the number of force computations that must be done.

Although these ideas are simply described, optimal performance on a vector machine requires careful attention to data structures and loop constructs to insure complete vectorization. The fastest implementation reported in the literature is that of Grest, et al. [24]. They use the combined neighbor list/link–cell method described above to create long lists of pairs of neighboring atoms. At each timestep, they prune the lists to keep only those pairs within the cutoff distance r_c. Finally, they organize the lists into packets in which no atom appears twice [45]. The force computation for each packet can then be completely vectorized, resulting

in performance on the benchmark problem described in Section 6 that is from 2 to 10 times faster than other vectorized algorithms [20, 30, 47] over a wide range of simulation sizes.

In recent years there has been considerable interest in devising parallel MD algorithms. The natural parallelism in MD is that the force calculations and velocity/position updates can be done simultaneously for all atoms. To date, two basic ideas have been exploited to achieve this parallelism. The goal in each is to divide the force computations in equation (1) evenly across the processors so as to extract maximum parallelism. To our knowledge, all algorithms that have been proposed or implemented (including ours) have been variations on these two methods. References [21, 25, 49] include good overviews of various techniques.

In the first class of methods a pre–determined set of force computations is assigned to each processor. The assignment remains fixed for the duration of the simulation. The simplest way of doing this is to give a subgroup of atoms to each processor. We call this method an *atom–decomposition* of the workload, since the processor computes forces on its atoms no matter where they move in the simulation domain. More generally, a subset of the force loops inherent in equation (1) can be assigned to each processor. We term this a *force–decomposition* and describe a new algorithm of this type later in the paper. Both of these decompositions are analogous to Lagrangian gridding in a fluids simulations where the grid cells (computational elements) move with the fluid (atoms in MD). By contrast, in the second general class of methods, which we call a *spatial–decomposition* of the workload, each processor is assigned a portion of the physical simulation domain. Each processor computes only the forces on atoms in its sub–domain. As the simulation progresses processors exchange atoms as they move from one sub–domain to another. This is analogous to an Eulerian gridding for a fluids simulation where the grid remains fixed in space as fluid moves through it.

Within the two classes of methods for parallelization of MD, a variety of algorithms have been proposed and implemented by various researchers. The details of the algorithms vary widely from one parallel machine to another since there are numerous problem–dependent and machine–dependent trade–offs to consider, such as the relative speeds of computation and communication. A brief review of some notable efforts follows.

Atom–decomposition methods, also called replicated–data methods [49] because identical copies of atom information are stored on all processors, are often used in MD simulations of molecular systems. This is because the duplication of information makes for straight–forward computation of additional three– and four–body force terms. Parallel implementations of state–of–the–art biological MD programs such as CHARMM and GROMOS using this technique are discussed in [13, 17]. Force–decomposition methods which systolically cycle atom data around a ring or through a grid of processors have been used on MIMD [26, 49] and SIMD machines [16, 57]. Other force–decomposition methods that use the force–matrix formalism we discuss in Sections 3 and 4 have been presented in [12] and [15]. Boyer and Pawley [12] decompose the force matrix by sub–blocks, while the method of Brunet, et al. [15] partitions the matrix element by element. In both cases their methods are designed for long–range force systems requiring all–pairs calculations (no neighbor lists) on SIMD machines. Thus the scaling of these algorithms is different from the algorithm presented in Section 4 as is the way they distribute the atom data among processors and perform inter–processor communication.

Spatial–decomposition methods, also called geometric methods [21, 25], are more common in the literature because they are well–suited to very large MD simulations. Recent parallel message–passing implementations for the Intel iPSC/2 hypercube [39, 46, 49], CM–5 [9, 51], Fujitsu AP1000 [14], and a T800 Transputer machine [20] have some features in common with the spatial–decomposition algorithm we present in Section 5. Our algorithm has the additional capability of working well in the regime where a processor's sub–domain is smaller than the force cutoff distance.

The fastest published algorithms for SIMD machines also employ spatial–decomposition techniques [52]. However, the data–parallel programming model, which on SIMD machines requires processors executing each statement to operate simultaneously on a global data structure, introduces inefficiencies in short–range MD algorithms, particularly when coding the construction and access of variable–length neighbor lists via indirect addressing. Thus the timings in [52] for the benchmark problem discussed in Section 6 on a 32K–processor CM–2 are slower than the single–processor Cray Y–MP timings presented in Section 7. By contrast, the timings for the message–passing parallel algorithms in this paper and references [9, 14, 51] are considerably faster, indicating the advantage a message–passing paradigm offers for exploiting parallelism in short–range MD simulations.

3   Atom–Decomposition Algorithm

In our first parallel algorithm each of the P processors is assigned a group of N/P atoms at the beginning of the simulation. Atoms in a group need not have any special spatial relationship to each other. For ease of exposition, we assume N is a multiple of P, though it is simple to relax this constraint. A processor will compute forces on only its N/P atoms and will update their positions and velocities for the duration of the simulation no matter where they move in the physical domain. As discussed in the previous section, this is an *atom–decomposition* (AD) of the computational workload.

A useful construct for representing the computational work involved in the algorithm is the $N \times N$ force matrix F. The (ij) element of F represents the force on atom i due to atom j. Note that F is sparse due to short–range forces and skew–symmetric, i.e. $F_{ij} = -F_{ji}$, due to Newton's 3rd law. We also define x and f as vectors of length N which store the position and total force on each atom. For a 3–D simulation, x_i would store the three coordinates of atom i. With these definitions, the AD algorithm assigns each processor a sub–block of F which consists of N/P rows of the matrix, as shown in Figure 1. If z indexes the processors from 0 to $P - 1$, then processor P_z computes matrix elements in the F_z sub–block of rows. It also is assigned the corresponding sub–vectors of length N/P denoted by x_z and f_z.

Assume the computation of matrix element F_{ij} requires only the two atom positions x_i and x_j. (We relax this assumption in Section 8.) To compute all the elements in F_z, processor P_z will need the positions of many atoms owned by other processors. In Figure 1 this is represented by having the horizontal vector x at the top of the figure span all the columns of F. This implies that every timestep each processor must receive updated atom positions from all the other processors, an operation called *all–to–all* communication. Various

algorithms have been developed for performing this operation efficiently on different parallel machines and architectures [7, 22, 54]. We use an idea outlined in Fox, et al. [22] that is simple, portable, and works well on a variety of machines. We describe it briefly because it is the chief communication component of both the AD algorithms of this section and the force–decomposition algorithms presented in the next section.

Following Fox's nomenclature, we term the all–to–all communication procedure an *expand* operation. Each processor allocates memory of length N to store the entire x vector. At the beginning of the expand, processor P_z has x_z, an updated piece of x of length N/P. Each processor needs to acquire all the other processor's pieces, storing them in the correct places in its copy of x. Figure 2a illustrates the steps that accomplish this for an 8–processor example. The processors are mapped consecutively to the sub–pieces of the vector. In the first communication step, each processor partners with an adjacent processor in the vector and they exchange sub–pieces. Processor 2 partners with 3. Now, every processor has a contiguous piece of x that is of length $2N/P$. In the second step, each processor partners with a processor two positions away and exchanges its new piece (2 receives the shaded sub–vectors from 0). Each processor now has a $4N/P$–length piece of x. In the last step, each processor exchanges an $N/2$–length piece of x with a processor $P/2$ positions away (2 exchanges with 6); the entire vector now resides on each processor.

A communication operation that is essentially the inverse of the expand will also prove useful in both the atom– and force–decomposition algorithms. Assume each processor has stored new force values throughout its copy of the force vector f. Processor P_z needs to know the N/P values in f_z, where each of the values is summed across all P processors. This is known as a *fold* operation [22] and is outlined in Figure 2b. In the first step each processor exchanges half the vector with a processor it partners with that is $P/2$ positions away. Note that each processor receives the half that it *is* a member of and sends the half it is *not* a member of (processor 2 receives the shaded first half of the vector from 6). Each processor sums the received values with its corresponding retained sub–vector. This operation is recursed, halving the length of the exchanged data at each step.

Costs for a communication algorithm are typically quantified by the number of messages and the total volume of data sent and received. On both these accounts the expand and fold of Figure 2 are optimal; each processor performs $\log_2(P)$ sends and receives and exchanges $N - N/P$ data values. Each processor also performs $N - N/P$ additions in the fold. A drawback is that the algorithms require $O(N)$ storage on every processor. Alternative methods for performing all–to–all communication require less storage at the cost of more sends and receives. This is usually not a good trade–off for MD simulations because, as we shall see, quite large problems can be run with the many Mbytes of local memory available on current–generation processors.

We now present two versions of an AD algorithm which use expand and fold operations. The first is simpler and does not take advantage of Newton's 3rd law. We call this algorithm **A1**; it is outlined in Figure 3 with the dominating term(s) in the computation or communication cost of each step listed on the right. We assume at the beginning of the timestep that each processor knows the current positions of all N atoms,

i.e. each has an updated copy of the entire x vector. Step (1) of the algorithm is to construct neighbor lists for all the pairwise interactions that must be computed in block F_z. Typically this will only be done once every few timesteps. If the ratio of the physical domain diameter D to the extended force cutoff length r_s is relatively small, it is quicker for P_z to construct the lists by checking all N^2/P pairs in its F_z block. When the simulation is large enough that 4 or more bins can be created in each dimension, it is quicker for each processor to bin all N atoms, then check the 27 surrounding bins of each of its N/P atoms to form the lists. This checking scales as N/P but has a large coefficient, so the overall scaling of the binned neighbor list construction is recorded as $N/P + N$.

In step (2) of the algorithm, the neighbor lists are used to compute the non−zero matrix elements in F_z. As each pairwise force interaction is computed, the force components are summed into f_z, so that F_z is never actually stored as a matrix. At the completion of the step, each processor knows the total force f_z on each of its N/P atoms. This is used to update their positions and velocities in step (4). (A step (3) will be added to other algorithms in this and the following sections.) Finally, in step (5) the updated atom positions in x_z are shared among all P processors in preparation for the next timestep via the expand operation of Figure 2a. As discussed above, this operation scales as N, the volume of data in the position vector x.

As mentioned above, algorithm **A1** ignores Newton's 3rd law. If different processors own atoms i and j as is usually the case, both processors compute the (ij) interaction and store the resulting force on their atom. This can be avoided at the cost of more communication by using a modified force matrix G which references each pairwise interaction only once. There are several ways to do this by striping the force matrix [48]; we choose instead to form G as follows. Let $G_{ij} = F_{ij}$, except that $G_{ij} = 0$ when $i > j$ and $i + j$ is even, and likewise $G_{ij} = 0$ when $i < j$ and $i + j$ is odd. Conceptually, G is colored like a checkerboard with red squares above the diagonal set to zero and black squares below the diagonal also set to zero. A modified AD algorithm **A2** that uses G to take advantage of Newton's 3rd law is outlined in Figure 4.

Step (1) is the same as in algorithm **A1** except only half as many neighbor list entries are made by each processor since G_z has only half the non−zero entries of F_z. This is reflected in the factors−of−two included in the scaling entries. For neighbor lists formed by binning, each processor must still bin all N atoms, but only need check half the surrounding bins of each of its N/P atoms. In step (2) the neighbor lists are used to compute elements of G_z. For an interaction between atoms i and j, the resulting forces on atoms i and j are summed into both the i and j locations of force vector f. This means each processor must store a copy of the entire force vector, as opposed to just storing f_z as in algorithm **A1**. When all the matrix elements have been computed, f is folded across all P processors using the algorithm in Figure 2b. Each processor ends up with f_z, the total forces on its atoms. Steps (4) and (5) then proceed the same as in **A1**.

Note that implementing Newton's 3rd law essentially halved the computation cost in steps (1) and (2), at the expense of doubling the communication cost. There are now two communication steps (3) and (5), each of which scale as N. This will only be a net gain if the communication cost in **A1** is less than a third of the overall run time. As we shall see, this will usually not be the case on large numbers of processors, so in

practice we almost always choose **A1** instead of **A2** for an AD algorithm. However, for small P or expensive force models, **A2** can be faster.

Finally, we discuss the issue of load–balance. Each processor will have an equal amount of work if each F_z or G_z block has roughly the same number of non–zero elements. This will be the case if the atom density is uniform across the simulation domain. However non–uniform densities can arise if, for example, there are free surfaces so that some atoms border on vacuum, or phase changes are occurring within a liquid or solid. This is only a problem for load–balance if the N atoms are ordered in a geometric sense as is typically the case. Then a group of N/P atoms near a surface, for example, will have fewer neighbors than groups in the interior. This can be overcome by randomly permuting the atom ordering at the beginning of the simulation, which is equivalent to permuting rows and columns of F or G. This insures that every F_z or G_z will have roughly the same number of non–zeros. A random permutation also has the advantage that the load–balance will likely persist as atoms move about during the simulation. Note that this permutation need only be done once, as a pre–processing step before beginning the dynamics.

In summary, the AD algorithms divide the MD force computation and integration evenly across the processors (ignoring the $O(N)$ component of binned neighbor list construction which is usually not significant). However, the algorithms require global communication, as each processor must acquire information held by all the other processors. This communication scales as N, independent of P, so it limits the number of processors that can be used effectively. The chief advantage of the algorithms is that of simplicity. Steps (1), (2), and (4) can be implemented by simply modifying the loops and data structures in a serial or vector code to treat N/P atoms instead of N. The expand and fold communication operations (3) and (5) can be treated as black–box routines and inserted at the proper locations in the code. Few other changes are typically necessary to parallelize an existing code.

4   Force–Decomposition Algorithm

Our next parallel MD algorithm is based on a block–decomposition of the force matrix rather than a row–wise decomposition as used in the previous section. We call this a *force–decomposition* (FD) of the workload. As we shall see, this improves the $O(N)$ scaling of the communication cost to $O(N/\sqrt{P})$. Block–decompositions of matrices are common in linear algebra algorithms for parallel machines [10, 28, 33] which sparked our interest in the idea, but to our knowledge we are the first to apply this idea to short–range MD simulations [29, 43, 42]. The assignment of sub–blocks of the force matrix to processors with a row–wise (calendar) ordering of the processors is depicted in Figure 5. We assume for ease of exposition that P is an even power of 2 and that N is a multiple of P, although again it is straightforward to relax these constraints. As before, we let z index the processors from 0 to $P-1$; processor P_z owns and will update the N/P atoms stored in the sub–vector x_z.

To reduce communication (explained below) the block–decomposition in Figure 5 is actually of a permuted force matrix F' which is formed by rearranging the columns of F in a particular way. If we order the x_z

pieces in row–order, they form the usual position vector x which is shown as a vertical bar at the left of the figure. Were we to have x span the columns as in Figure 1, we would form the force matrix as before. Instead, we span the columns with a permuted position vector x', shown as a horizontal bar at the top of Figure 5, in which the x_z pieces are stored in *column–order.* Thus, in the 16–processor example shown in the figure, x stores each processor's piece in the usual order $(0, 1, 2, 3, 4, ..., 14, 15)$ while x' stores them as $(0, 4, 8, 12, 1, 5, 9, 13, 2, 6, 10, 14, 3, 7, 11, 15)$. Now the (ij) element of F' is the force on atom i in vector x due to atom j in permuted vector x'.

The F'_z sub–block owned by each processor P_z is of size $(N/\sqrt{P}) \times (N/\sqrt{P})$. To compute the matrix elements in F'_z, processor P_z must know one $N/\sqrt{P}$–length piece of each of the x and x' vectors, which we denote as x_α and x'_β. As these elements are computed they will be accumulated into corresponding force sub–vectors f_α and f'_β. The Greek subscripts α and β each run from 0 to $\sqrt{P} - 1$ and reference the row and column position occupied by processor P_z. Thus for processor 6 in the figure, x_α consists of the x sub–vectors $(4, 5, 6, 7)$ and x'_β consists of the x' sub–vectors $(2, 6, 10, 14)$.

Our first FD algorithm **F1** is outlined in Figure 6. As before, each processor has updated copies of the needed atom positions x_α and x'_β at the beginning of the timestep. In step (1) neighbor lists are constructed. Again, for small problems this is most quickly done by checking all N^2/P possible pairs in F'_z. For large problems, the $N/\sqrt{P}$ atoms in x'_β are binned, then the 27 surrounding bins of each atom in x_α is checked. The total number of interactions stored in each processor's lists is still $O(N/P)$. The scaling of the binned neighbor list construction is thus $N/P + N/\sqrt{P}$. In step (2) the neighbor lists are used to compute the matrix elements in F'_z. As before the elements are summed into a local copy of f_α as they are computed, so F'_z never need be stored in matrix form. In step (3) a fold operation is performed within each row of processors so that processor P_z obtains the total forces f_z on its N/P atoms. Although the fold algorithm used is the same as in the preceding section, there is a key difference. In this case the vector f_α being folded is only of length $N/\sqrt{P}$ and only the $\sqrt{P}$ processors in one row are participating in the fold. Thus this operation scales as $N/\sqrt{P}$ instead of N as in the AD algorithm.

In step (4), f_z is used by P_z to update the N/P atom positions in x_z. Steps (5a-5b) share these updated positions with all the processors that will need them for the next timestep. These are the processors which share a row or column with P_z. First, in (5a), the processors in row α perform an expand of their x_z sub–vectors so that each acquires the entire x_α. As with the fold, this operation scales as the $N/\sqrt{P}$ length of x_α instead of as N as it did in algorithms **A1** and **A2**. Similarly, in step (5b), the processors in each column β perform an expand of their x_z. As a result they all acquire x'_β and are ready to begin the next timestep.

It is in step (5) that using a permuted force matrix F' saves extra communication. The permuted form of F' causes x_z to be a component of both x_α and x'_β for each P_z. This would not be the case if we had block–decomposed the original force matrix F by having x span the columns instead of x'. Then in Figure 5 the x_β for P_6 would have consisted of the sub–vectors $(8, 9, 10, 11)$, none of which components are known by

P_6. Thus, before performing the expand in step (5b), processor 6 would need to first acquire one of these 4 components from another processor (in the transpose position in the matrix [29]), requiring an extra $O(N/P)$ communication step. The transpose–free version of the FD algorithms presented here was motivated by a matrix permutation for parallel matrix–vector multiplication discussed in reference [33].

As with algorithm **A1**, algorithm **F1** does not take advantage of Newton's 3rd law; each pairwise force interaction is computed twice. Algorithm **F2** avoids this duplicated effort by checkerboarding the force matrix as in the preceding section. Specifically, the checkerboarded matrix G is permuted in the same way as F was, to form G'. Note that now the total force on atom i is the sum of all matrix elements in row i minus the sum of all elements in column i. The modified FD algorithm **F2** is outlined in Figure 7. Step (1) is the same as in F1, except that half as many interactions are stored in the neighbor lists. Likewise, step (2) requires only half as many matrix elements be computed. For each (ij) element, the computed force components are now summed into two force sub–vectors instead of one. The force on atom i is summed into f_α in the location corresponding to row i. Likewise, the force on atom j is summed into f'_β in the location corresponding to column j. Steps (3a-3c) accumulate these forces so that processor P_z ends up with the total force on its N/P atoms. First, in step (3a), the $\sqrt{P}$ processors in column β fold their local copies of f'_β. The result is f'_z. Each element of this N/P–length sub–vector is the sum of an entire column of G'. Next, in step (3b), the row contributions to the forces are summed by performing a fold of the f_α vector within each row α. The result is f_z, each element of which is the sum across a row of G'. Finally, in step (3c) the column and row contributions are subtracted element by element to yield the total forces f_z on the atoms owned by processor P_z. The processor can now update the positions and velocities of its atoms; steps 4 and 5 are identical to those of **F1**.

In the FD algorithms, exploiting Newton's 3rd law again halves the computation required in steps (1) and (2). However, the communication cost in steps (3) and (5) does not double. Rather there are 4 expands and folds required in **F2** versus 3 in **F1**. Thus, in practice, it is usually faster to use algorithm **F2** with its reduced computational cost and slightly increased communication cost rather than **F1**. The key point is that all the expand and fold operations in **F1** and **F2** scale as $N/\sqrt{P}$ rather than as N as was the case in algorithms **A1** and **A2**. As we shall see, when run on large numbers of processors this significantly reduces the time the FD algorithms spend on communication as compared to the AD algorithms.

Finally, the issue of load–balance is a more serious concern for the FD algorithms. Processors will have equal work to do only if all the matrix blocks F'_z or G'_z are uniformly sparse. If the atoms are ordered geometrically this will not be the case even for problems with uniform density. This is because such an ordering creates a force matrix with diagonal bands of non–zero elements. As in the AD case, a random permutation of the atom ordering produces the desired effect. Only now the permutation should be done as a pre–processing step for all problems, even those with uniform atom densities.

In summary, algorithms **F1** and **F2** divide the MD computations evenly across processors as did the AD algorithms. But the block–decomposition of the force matrix means each processor only needs $O(N/\sqrt{P})$

information to perform its computations. Thus the communication and memory costs are reduced by a factor of $\sqrt{P}$ versus algorithms **A1** and **A2**. The FD strategy retains the simplicity of the AD technique; **F1** and **F2** can be implemented using the same "black–box" communication routines as **A1** and **A2**. The FD algorithms also need no geometric information about the physical problem being modeled to perform optimally. In fact, for load–balancing purposes the algorithms intentionally ignore such information by using a random atom ordering.

5   Spatial–Decomposition Algorithm

In our final parallel algorithm the physical simulation domain is subdivided into small 3–D boxes, one for each processor. We call this a *spatial–decomposition* (SD) of the workload. Each processor computes forces on and updates the positions and velocities of all atoms within its box at each timestep. Atoms are reassigned to new processors as they move through the physical domain. In order to compute forces on its atoms, a processor need only know positions of atoms in nearby boxes. The communication required in the SD algorithm is thus local in nature as compared to global in the AD and FD cases.

The size and shape of the box assigned to each processor will depend on N, P, and the aspect ratio of the physical domain, which we assume to be a 3–D rectangular parallelepiped. Within these constraints the number of processors in each dimension is chosen so as to make each processor's box as "cubic" as possible. This is to minimize communication since in the large N limit the communication cost of the SD algorithm will turn out to be proportional to the surface area of the boxes. An important point to note is that in contrast to the link–cell method described in Section 2, the box lengths may now be smaller or larger than the force cutoff lengths r_c and r_s.

Each processor in our SD algorithm maintains two data structures, one for the N/P atoms in its box and one for atoms in nearby boxes. In the first data structure, each processor stores complete information — positions, velocities, neighbor lists, etc. This data is stored in a linked list to allow insertions and deletions as atoms move to new boxes. In the second data structure only atom positions are stored. Interprocessor communication at each timestep keeps this information current.

The communication scheme we use to acquire this information from processors owning the nearby boxes is shown in Figure 8. The first step (a) is for each processor to exchange information with adjacent processors in the east/west dimension. Processor 2 fills a message buffer with atom positions it owns that are within a force cutoff length r_s of processor 1's box. (The reason for using r_s instead of r_c will be made clear below.) If $d < r_s$, where d is the box length in the east/west direction, this will be all of processor 2's atoms; otherwise it will be those nearest to box 1. Now each processor sends its message to the processor in the westward direction (2 sends to 1) and receives a message from the eastward direction. Each processor puts the received information into its second data structure. Now the procedure is reversed with each processor sending to the east and receiving from the west. If $d > r_s$, all needed atom positions in the east–west dimension have now been acquired by each processor. If $d < r_s$, the east–west steps are repeated with each processor sending

more needed atom positions to its adjacent processors. For example, processor 2 sends processor 1 atom positions from box 3 (which processor 2 now has in its second data structure). This can be repeated until each processor knows all atom positions within a distance r_s of its box, as indicated by the dotted boxes in the figure. The same procedure is now repeated in the north/south dimension; see step (b) of the figure. The only difference is that messages sent to the adjacent processor now contain not only atoms the processor owns (in its first data structure), but also any atom positions in its second data structure that are needed by the adjacent processor. For $d = r_s$ this has the effect of sending 3 boxes worth of atom positions in one message as shown in (b). Finally, in step (c) the process is repeated in the up/down dimension. Now atom positions from an entire plane of boxes (9 in the figure) are being sent in each message.

There are several key advantages to this scheme, all of which reduce the overall cost of communication in our algorithm. First, for $d \geq r_s$, needed atom positions from all 26 surrounding boxes are obtained in just 6 data exchanges. Moreover, as will be discussed in Section 7, if the parallel machine is a hypercube, the processors can be mapped to the boxes in such a way that all 6 of these processors will be directly connected to the center processor. Thus message passing will be fast and contention–free. Second, when $d < r_s$ so that atom information is needed from more distant boxes, this occurs with only a few extra data exchanges, all of which are still with the 6 immediate neighbor processors. This is an important feature of the algorithm which enables it to perform well even when large numbers of processors are used on relatively small problems.

A third advantage is that the amount of data communicated is minimized. Each processor acquires only the atom positions that are within a distance r_s of its box. Fourth, all of the received atom positions can be placed as contiguous data directly into the processor's second data structure. No time is spent rearranging data, except to create the buffered messages that need to be sent. Finally, as will be discussed in more detail below, this message creation can be done very quickly. A full scan of the two data structures is only done once every few timesteps, when the neighbor lists are created, to decide which atom positions to send in each message. The scan procedure creates a list of atoms that make up each message. During all the other timesteps, the lists can be used, in lieu of scanning the full atom list, to directly index the referenced atoms and buffer up the messages quickly. This is the equivalent of a gather operation on a vector machine.

We now outline our SD algorithm **S1** in Figure 9. Box z is assigned to processor P_z, where z runs from 0 to $P - 1$ as before. Processor P_z stores the atom positions of its N/P atoms in x_z and the forces on those atoms in f_z. Steps (1a-1c) are the neighbor list construction, performed once every few timesteps. This is somewhat more complex than in the other algorithms because, as discussed above, it includes the creation of lists of atoms that will be communicated at every timestep. First, in step (1a) the positions, velocities, and any other identifying information of atoms that are no longer inside box z are deleted from x_z (first data structure) and stored in a message buffer. These atoms are exchanged with the 6 adjacent processors via the communication pattern of Figure 8. As the information routes through each dimension, processor P_z checks for new atoms that are now inside its box boundaries, adding them to its x_z. Next, in step (1b),

14

all atom positions within a distance r_s of box z are acquired by the communication scheme described above. As the different messages are buffered by scanning through the two data structures, lists of included atoms are made. The lists will be used in step (5). The scaling factor Δ for steps (1a) and (1b) will be explained below.

When steps (1a) and (1b) are complete, both of the processor's data structures are current. Neighbor lists for its N/P atoms can now be constructed in step (1c). If atoms i and j are both in box z (an inner−box interaction), the (ij) pair is only stored once in the neighbor list. If i and j are in different boxes (a two−box interaction), both processors store the interaction in their respective neighbor lists. If this were not done, processors would compute forces on atoms they do not own and communication of the forces back to the processors owning the atoms would be required. A modified algorithm which performs this communication to avoid the duplicated force computation of two−box interactions is discussed below. When d, the length of box z, is less than two cutoff distances, it is quicker to find neighbor interactions by checking each atom inside box z against all the atoms in both of the processor's data structures. This scales as the square of N/P. If $d > 2r_s$, then with the shell of atoms around box z, there are 4 or more bins in each dimension. In this case, as with the algorithms of the preceding sections, it is quicker to perform the neighbor list construction by binning. All the atoms in both data structures are mapped to bins of size r_s. The surrounding bins of each atom in box z are then checked for possible neighbors.

Processor P_z can now compute all the forces on its atoms in step (2) using the neighbor lists. When the interaction is between two atoms inside box z, the resulting force is stored twice in f_z, once for atom i and once for atom j. For two−box interactions, only the force on the processor's own atom is stored. After computing f_z, the atom positions are updated in step (4). Finally, these updated positions must be communicated to the surrounding processors in preparation for the next timestep. This occurs in step (5) in the communication pattern of Figure 8 using the previously created lists. The amount of data exchanged in this operation is a function of the relative values of the force cutoff distance and box length and is discussed in the next paragraph. Also, we note that on the timesteps that neighbor lists are constructed, step (5) does not have to be performed since step (1b) has the same effect.

The communication operations in algorithm **S1** occur in steps (1a), (1b), and (5). The communication in the latter two steps is identical. The cost of these steps scales as the volume of data exchanged. For step (5), if we assume uniform atom density, this is proportional to the physical volume of the shell of thickness r_s around box z, namely $(d + 2r_s)^3 - d^3$. Note there are roughly N/P atoms in a volume of d^3, since d^3 is the size of box z. There are 3 cases to consider. First, if $d < r_s$ data from many neighboring boxes must be exchanged and the operation scales as $8r_s{}^3$. Second, if $d \approx r_s$, the data in all 26 surrounding boxes is exchanged and the operation scales as $27N/P$. Finally, if d is much larger than r_s, only atom positions near the 6 faces of box z will be exchanged. The communication then scales as the surface area of box z, namely $6r_s(N/P)^{2/3}$. These 3 cases are explicitly listed in the scaling of step (5). Elsewhere in Figure 9, we use the term Δ to represent whichever of the three is applicable for a given N, P, and r_s. We note that step (1a)

involves less communication since not all the atoms within a cutoff distance of a box face will move out of the box. But this operation still scales as the surface area of box z, so we list its scaling as Δ.

The computational portion of algorithm **S1** is in steps (1c), (2), and (4). All of these scale as N/P with additional work in steps (1c) and (2) for atoms that are neighboring box z and stored in the second data structure. The number of these atoms is proportional to Δ so it is included in the scaling of those steps. The leading term in the scaling of steps (1c) and (2) is listed as $N/2P$ as in algorithms **A2** and **F2**, since inner–box interactions are only stored and computed once for each pair of atoms in algorithm **S1**. Note that as d grows large relative to r_s as it will for very large simulations, the Δ contribution to the overall computation time decreases and the overall scaling of algorithm **S1** approaches the optimal $N/2P$. In essence, each processor spends nearly all its time working in its own box and only exchanges a relatively small amount of information with neighboring processors to update its boundary conditions.

An important feature of algorithm **S1** is that the data structures are only modified once every few timesteps when neighbor lists are constructed. In particular, even if an atom moves outside box z's boundaries it is not reassigned to a new processor until step (1a) is executed [51]. Processor P_z can still compute correct forces for the atom so long as two criteria are met. The first is that an atom does not move farther than d between two neighbor list constructions. The second is that all nearby atoms within a distance r_s, instead of r_c, must be updated every timestep. The alternative is to move atoms to their new processors at every timestep [41]. This has the advantage that only atoms within a distance r_c of box z need be exchanged at all timesteps when neighbor lists are not constructed. This reduces the volume of communication since $r_c < r_s$. However, now the neighbor list of a reassigned atom must also be sent. The information in the neighbor list is atom indices referencing local memory locations where the neighbor atoms are stored. If atoms are continuously moving to new processors, these local indices become meaningless. To overcome this, our implementation in [41] assigned a global index (1 to N) to each atom which moved with the atom from processor to processor. A mapping of global index to local memory must then be stored in a vector of size N by each processor or the global indices must be sorted and searched to find the correct atoms when they are referenced in a neighbor list. The former solution limits the size of problems that can be run; the latter solution incurs an extra cost for the sort and search operations. We found that implementing the Tamayo and Giles idea [51] in our algorithm **S1** made the resulting code less complex and reduced the computational and communication overhead. This did not affect the timings for simulations with large N, but improved the algorithm's performance for medium–sized problems.

A modified version of **S1** that takes full advantage of Newton's 3rd law can also be devised, call it algorithm **S2**. If processor P_z acquires atoms only from its west, south, and down directions (and sends its own atoms only in the east, north, and up directions), then each pairwise interaction need only be computed once, even when the two atoms reside in different boxes. This requires sending computed force results back in the opposite directions to the processors who own the atoms, as a step (3) in the algorithm. This scheme does not reduce communication costs, since half as much information is communicated twice as often, but

does eliminate the duplicated force computations for two–box interactions. An algorithm similar to this is detailed in [14] for the Fujitsu AP1000 machine with results that we highlight in the next section. Two points are worth noting. First, the overall savings of **S2** over **S1** is small, particularly for large N. Only the Δ term in steps (1c) and (2) is saved. Second, as we will show in Section 7, the performance of SD algorithms for large systems can be improved by optimizing the single–processor force computation in step (2). As with vector machines this requires more attention be paid to data structures and loop orderings in the force and neighbor–list construction routines to achieve high single–processor flop rates. Implementing **S2** requires special–case coding for atoms near box edges and corners to insure all interactions are counted only once [14] which can hinder this optimization process.

Finally, the issue of load–balance is an important concern in any SD algorithm. Algorithm **S1** will be load–balanced only if all boxes have a roughly equal number of atoms (and surrounding atoms). This will not be the case if the physical atom density is non–uniform. Additionally, if the physical domain is not a rectangular parallelepiped, it can be difficult to split into P equal–sized pieces. Sophisticated load–balancing algorithms have been developed [27] to partition an irregular physical domain or non–uniformly dense clusters of atoms, but they create sub–domains which are irregular in shape or are connected in an irregular fashion to their neighboring sub–domains. In either case, the task of assigning atoms to sub–domains and communicating with neighbors becomes more costly and complex. If the physical atom density changes over time during the MD simulation, the load–balance problem is compounded. Any dynamic load–balancing scheme requires additional computational overhead and data movement.

In summary, the SD algorithm, like the AD and FD algorithms, evenly divides the MD computations across all the processors. Its chief benefit is that it takes full advantage of the local nature of the interatomic forces by performing only local communication. Thus, in the large N limit, it achieves optimal $O(N/P)$ scaling and is clearly the fastest algorithm. However, this is only true if good load–balance is also achievable. Since its performance is sensitive to the problem geometry, algorithm **S1** is more restrictive than **A2** and **F2** whose performance is geometry–independent. A second drawback of algorithm **S1** is its complexity; it is more difficult to implement efficiently than the simpler AD and FD algorithms. In particular the communication scheme requires extra coding and bookkeeping to create messages and access data received from neighboring boxes. In practice, integrating algorithm **S1** into an existing serial MD code can require a substantial reworking of data structures and code.

6   Benchmark Problem

The test case used to benchmark our three parallel algorithms is a MD problem that has been used extensively by various researchers [9, 14, 20, 24, 30, 41, 47, 51, 52]. It models atom interactions with a Lennard–Jones potential energy between pairs of atoms separated by a distance r as

$$\Phi(r) = 4\epsilon \left[(\frac{\sigma}{r})^{12} - (\frac{\sigma}{r})^6 \right] \tag{2}$$

where ϵ and σ are constants. The derivative of this energy expression with respect to r is the F_2 term in equation (1); F_3 and higher-order terms are ignored.

The N atoms are simulated in a 3–D parallelepiped with periodic boundary conditions at the Lennard Jones state point defined by the reduced density $\rho^* = 0.8442$ and reduced temperature $T^* = 0.72$. This is a liquid state near the Lennard–Jones triple point. The simulation is begun with the atoms on an *fcc* lattice with randomized velocities. The solid quickly melts as the system evolves to its natural liquid state. A roughly uniform spatial density persists for the duration of the simulation. The simulation is run at constant N, volume V, and energy E, a statistical sampling from the microcanonical ensemble. Force computations using the potential in equation (2) are truncated at a distance $r_c = 2.5\sigma$. The integration timestep is 0.00462 in reduced units. For simplicity we use a leapfrog scheme to integrate equation (1) as in [2]. Other implementations of the benchmark [24] have used predictor–corrector schemes; this only slows their performance by 2–3%.

For timing purposes, the critical features of the benchmark for a given problem size N are ρ^* and r_c. These determine how many force interactions must be computed at every timestep. The number of atoms in a sphere of radius $r^* = r/\sigma$ is given by $4\pi\rho^*(r^*)^3/3$. For this benchmark, using $r_c = 2.5\sigma$, each atom has on average 55 neighbors. If neighbor lists are used, the benchmark also defines an extended cutoff length $r_s = 2.8\sigma$ (encompassing about 78 atoms) for forming the neighbor lists and specifies that the lists be created or updated every 20 timesteps. Timings for the benchmark are usually reported in CPU seconds/timestep. If neighbor lists are used then the cost of creating them every 20 steps is amortized over the per timestep timing.

It is worth noting that without running a standard benchmark problem it can be difficult to accurately assess the performance of a parallel algorithm. In particular, it can be misleading to only compare performance of a parallel version of a code to the original vectorized or serial code because, as we have learned from our codes as well as other's results, the vector code performance may well be far from optimal. Even when problem specifications are reported, it can be difficult to compare two algorithm's relative performance when two different benchmark problems are used. This is because of the wide variability in the cost of calculating force equations, the number of neighbors included in cutoff distances, and the frequency of neighbor list building as a function of temperature, atom density, cutoff distances, etc.

7 Results

The parallel algorithms of Sections 3, 4, and 5 were tested on several MIMD parallel supercomputers capable of message–passing programming, a nCUBE 2, an Intel iPSC/860 and Intel Paragon, and a Cray T3D. The first three machines are at Sandia; the T3D is at Cray Research. The nCUBE 2 is a 1024–processor

hypercube. Each processor is a custom scalar chip capable of about 2 Mflops peak and has 4 Gbytes of memory. The communications bandwidth between processors is 2 Mbytes/sec. Sandia's iPSC/860 has 64 i860XR processors connected in a hypercube topology. Its processors have 8 Mbytes of memory and are capable of about 60 Mflops peak, but in practice 4–7 Mflops is the typical compiled Fortran performance. Communications bandwidth on the iPSC/860 is 2.7 Mbytes/sec. The Intel Paragon at Sandia has from 1840 to 1904 processors which are connected as a 2–D mesh. The individual i860XP processors have 16 Mbytes of memory and are about 30% faster than those in the iPSC/860. The Paragon communication bandwidth is 150 Mbytes/sec peak, but in practice is a function of message length and data alignment. The Cray T3D used in this study has 512 processors connected as a 3–D torus, each with 64 Mbytes of memory. Its processors are DEC Alpha (RISC) chips capable of 150 Mflops peak with typical compiled Fortran performance of 15–20 Mflops. The T3D communications bandwidth is 165 Mbytes/sec peak.

Because the algorithms were implemented in standard Fortran with calls to vendor–supplied message-passing subroutines (sends and receives), only minor changes were required to implement the benchmark codes on the different machines. As described, the algorithms do not specify a mapping of physical processors to logical computational elements (force matrix sub–blocks, 3–D boxes). An optimal mapping would be tailored to a particular machine architecture so as to minimize message contention (multiple messages using the same communication wire) and the distance messages have to travel between pairs of processors that are not directly connected by a communication wire. The mappings we use are near–optimal and conceptually simple.

For the atom–decomposition (AD) algorithm we simply assign the processors in ascending order to the row–blocks of the force matrix as in Figure 1. The expands and folds then take place exactly as in Figure 2. On the hypercube machines (nCUBE and iPSC/860) this is optimal; on the mesh machines (Paragon and T3D) some messages will (unavoidably) be exchanged between non–neighbor processors. For the force-decomposition (FD) algorithm we use a natural calendar ordering of the processors in the permuted force matrix as in Figure 5. On a hypercube this means each row and column of the matrix is a sub–cube of processors so that expands and folds within rows and columns can be done optimally. On a 2–D mesh (Paragon), all the communication is within rows and columns of processors, until we use so many processors that (for example) 16x64 physical processors are configured as a 32x32 logical mesh.

For the spatial–decomposition (SD) algorithm on the hypercube machines we use a processor mapping that configures the hypercube as a 3–D torus. Such a mapping is done using a Gray–coded ordering [22] of the processors. This insures each processor's box in Figure 8 has 6 spatial neighbors (boxes in the east, west, north, south, up, down directions) that are assigned to processors which are also nearest neighbors in the hypercube topology. Communication with these neighbors is thus contention–free. Gray-coding also provides naturally for periodic boundary conditions in the MD simulation since processors at the edge of the 3–D torus are topological nearest neighbors to those on the opposite edge. On the Paragon we assign planes of boxes in the 3–D domain to contiguous subsets of the 2–D mesh of processors; data exchanges in

the 3rd dimension thus (unavoidably) require non–nearest–neighbor communication. On the Cray T3D the physical 3–d domain maps naturally to the 3–d torus of processors.

Timing results for the benchmark problem on the different parallel machines are shown in Tables I, II, and III for the AD, FD, and SD algorithms. A wide range of problem sizes are considered from $N = 500$ atoms to $N = 10^8$ atoms. The lattice size for each problem is also specified; there are 4 atoms per unit cell for the initial–state fcc lattices. Entries with a dashed line are for problems that would not fit in available memory. The 100,000,000 atom problem nearly filled the 30 Gbytes of memory on the 1904–processor Paragon with neighbor lists consuming the majority of the space.

For comparison, we also implemented the vectorized algorithm of Grest, et al. [24] on single processors of Sandia's Cray Y–MP and a Cray C90 at Cray Research. Our version is only slightly different from the original Grest code, using a simpler integrator and allowing for non–cubic physical domains. The timings in reference [24] were for a Cray X–MP. We believe these timings for the faster Y–MP and C90 architectures are the fastest that have been reported for this benchmark problem on a single processor of a conventional vector supercomputer. They show a C90 processor to be about 2.5 times faster than a Y–MP processor for this algorithm. The starred Cray timings in the tables are estimates for problems too large to fit in memory on the machines accessible to us. They are extrapolations of the $N = 10^5$ system timing based on the observed linear scaling of the Cray algorithm. It is also worth noting that ideas similar to those used in the parallel algorithms of the previous sections could be used to create efficient parallel Cray codes for multiple processors of a Y–MP or C90. For example, a speed–up of 6.8 on a 8–processor Cray Y–MP has been achieved by Attig and Kremer with the Grest, et al. algorithm [3].

Finally, we have also implemented specially optimized versions of the SD algorithm on the Intel Paragon. Performance numbers for these codes are shown in Table IV. The first enhancement takes advantage of the fact that each "node" of the Paragon actually has two i860 processors, one for computation and one for communication. An option under the SUNMOS operating system [35] run on Sandia's Paragon is to use the second processor for computation. This requires minor coding changes to stride the loops in the force and neighbor routines so that each processor can perform independent computations (without writing to the same memory location) simultaneously. The speed-up due to this enhancement is less than a factor of two, since both processors are competing for bus bandwidth to memory. The second enhancement was more work; it involved writing an i860 assembler version (see acknowledgments) of the most critical computational kernel, the force computation, which takes 70 to 80% of the time for large problems. The assembler routine is about 2.5 times faster than its Fortran counterpart, yielding an overall speed–up of about 1.75 on large problems. These enhancements can be combined (minus an overhead factor due to bus competition) to yield the fastest version of the code with a speed–up of nearly 3 over the original Fortran code.

The parallel timings in all of the tables for the nCUBE and Intel machines are for single–precision (32–bit) implementations of the benchmark. The Y–MP, C90, and T3D timings are for 64–bit arithmetic since that is the only option. MD simulations do not typically require double precision accuracy since there is a

20

Table I: CPU seconds/timestep for the atom–decomposition algorithm **A1** on several parallel machines for the benchmark simulation. Single processor Cray Y–MP and C90 timings using a fully vectorized algorithm are also given for comparison.

much coarser approximation inherent in the potential model and the integrator. This is particularly true of Lennard–Jones systems since the ϵ and σ coefficients are only specified to a few digits of accuracy as an approximate model of the interatomic energies in a real material. With this said, double precision timings can be easily estimated. The processors in the nCUBE and Intel machines compute about 20–30% slower in double–precision arithmetic than single, so the time spent computing would be increased by that amount. Communication costs in each of the algorithms would essentially double, since the volume of information being exchanged in messages would increase by a factor of two. Thus depending on the fraction of time being spent in communication for a particular N and P (see the scaling discussion below), the overall timings typically increase by 20–50% for double–precision runs.

The tables show the parallel machines to be competitive with the Cray Y–MP and C90 machines across the entire range of problem sizes for all three parallel algorithms. The FD algorithm is fastest for the smallest problem sizes; SD is fastest for large N. For the Fortran version of the code the Cray T3D is the fastest of the parallel machines on a per–processor basis; overall the Intel Paragon is the fastest. On 1840 dual–processor nodes of the Paragon (3680 i860 processors) the assembler–optimized SD code is 415 times faster than a

Table II: CPU seconds/timestep for the force–decomposition algorithm **F2** on several parallel machines and the Cray Y–MP and C90.

single Y–MP processor on the largest problem sizes and 165 times faster than a C90 processor. A surprising result is that the parallel machines are competitive with a single processor of the Cray machines even for the smallest problem sizes. One typically does not think of there being enough parallelism to exploit when there are only a few atoms per processor.

The floating point operation (flop) rate for the parallel codes can also be estimated. Computing the force between two interacting atoms requires 23 flops with an average of 27.6 interactions per atom (taking into account Newton's 3rd law) computed each timestep for the benchmark. This gives a total flop rate for the Fortran code of 6.97 Gflops for the 100,000,000 atom problem on 1904 processors of the Paragon. The dual–processor assembler–optimized version runs the same problem at 18.0 Gflops on 1840 nodes. By comparison the C90 processor is running at 107 Mflops for large N though its hardware performance monitor reports a rate of over 200 Mflops. The difference is that both the vector and parallel codes perform flops to set up neighbor lists and check atom distances that end up outside the force cutoff; we are not counting them in these figures since they do not contribute to the answer.

Large N timings for this benchmark on other parallel machines are discussed in [9, 14, 20, 52], all for SD algorithms. The best timings on SIMD machines are reported by Tamayo, et al. [52] who implemented

22

Table III: CPU seconds/timestep for the spatial–decomposition algorithm **S1**.

several data–parallel algorithms on a 32K–processor CM–2 (1024 floating point processors). Their fastest algorithm ran at 0.57 sec/timestep for a $N = 18000$ atom system, about a factor of two slower than the single processor Y–MP timing in the tables here. Brown, et al. [14] detail a message–passing algorithm similar to the **S2** algorithm discussed in Section 5. For a $N = 729000$ atom system (at a slightly smaller density of $\rho^* = 0.8$) run on 512 processors of the Fujitsu AP1000 they report a time of 0.927 sec/timestep. Esselink, et al. [20] report a time of 0.86 sec/timestep for a $N = 39304$ atom system (at a smaller density of $\rho^* = 0.7$) on a 400 processor T800 Transputer system. Finally, Beazley, et al. [9] report timings of 0.44 sec/timestep for a $N = 1,024,000$ atom system and 16.55 sec/timestep for a $N = 65,536,000$ atom system (both at a higher density of $\rho^* = 1.0$) run on a 1024–node CM–5. (Their current timings are about 15% faster [34]). The latter run is at a rate of 28 Gflops, but a large fraction of these flops are computed on atoms outside the force cutoff and they count 35 flops/interaction. Their algorithm does not use neighbor lists so as to enable faster performance of assembler routines on the CM–5 vector units; without the memory overhead for neighbor lists they have simulated systems with up to 180,000,000 atoms.

The timings in Table I show that communication costs have begun to dominate in the AD algorithm by the time hundreds of processors are used. There is little speed gained by doubling the number of processors. By contrast timings in Table II show the FD algorithm is speeding up by roughly 30% when the number

23

of processors is doubled. The timings for the largest problem sizes in Table III evidence excellent scaling properties even on relatively small problems when there are only a few atoms per processor. Doubling P nearly halves the run times for a given N. Similarly, as N increases for fixed P, the run times per atom actually become faster as the surface–to–volume ratio of each processor's box is reduced. We note, however, that this scaling depends on uniform atom density within a simple domain such as the rectangular parallelepiped of the benchmark problem.

The algorithm's relative performance can be better seen in graphical form using data from all 3 tables. Figure 10 shows a 1024–processor Paragon's performance on the benchmark simulation as a function of problem size. Single processor Y–MP and C90 timings are also included. The linear scaling of all the algorithms in the large N limit is evident. Note that FD is faster than AD across all problem sizes due to its reduced communication costs. On this many processors, the SD algorithm has significant overhead costs for small N. This is because the d/r_s ratio is so small that each processor has to communicate with a large number of neighboring processors to acquire all its needed information. As N increases, this overhead is reduced relative to the computation performed inside the processor's box, and the algorithm's performance asymptotically approaches its optimal $O(N/P)$ performance. Thus there is a cross–over size N at which the SD algorithm becomes faster than FD. For this benchmark it is at about 4 atoms/processor indicating that the spatial algorithm is still working quite well even when the box size is small relative to the force cutoff.

In Figure 11 we plot the nCUBE 2's performance on the $N = 10976$ atom benchmark as a function of number of processors for two different cutoff lengths, 2.5σ (solid symbols) and 5.0σ (open symbols). Single processor Y–MP and C90 timings are also shown for the 2.5σ benchmark. The dotted lines are the maximum achievable speed of the nCUBE if any of the algorithms were 100% efficient. Parallel efficiency is defined as the run time on 1 processor divided by the quantity ($P \times$ run time on P processors). Thus if the 512–processor timing is 256 times as fast as the 1–processor timing, the algorithm is 50% efficient. On small numbers of processors communication is not a significant factor and all the algorithms perform similarly; as P increases, the algorithms become less efficient. The AD algorithm falls off most rapidly due to the $O(N)$ scaling of its communication. For the 2.5σ case, FD is next most efficient due to its $O(N/\sqrt{P})$ communication scaling. When hundreds of processors are used, even the SD algorithm becomes less efficient since now the box size is small relative to the force cutoff distance for this N. For the longer cutoff case (more typical of what might be used in an organic system simulation with Coulombic forces), the FD algorithm is actually faster than SD for all P. This is because the communication cost in the AD and FD algorithms is independent of the cutoff length, unlike the SD case.

Using one–processor timings as reference points, parallel efficiencies can be computed for all the algorithms or, equivalently, the fraction of time spent in communication in each of the entries in Tables I, II, and III. Running the largest problems that fit in memory on a single processor of each of the parallel machines gave timings on the Cray T3D, nCUBE 2, and Intel iPSC/860 and Paragon of 8.23×10^{-5}, 9.15×10^{-4}, 2.03×10^{-4}, and 1.57×10^{-4} seconds/timestep/atom respectively. By comparison, single–processor Cray Y–MP and C90

timings are 1.47×10^{-5} and 5.92×10^{-6} seconds/timestep/atom. Combining these results with the Table III timings for the $N = 1,000,000$ atom simulation show the SD algorithm **S1** has a parallel efficiency of 76% and 77% on 1024 processors of the nCUBE 2 and Intel Paragon and 78% on 512 processors of the Cray T3D. The largest simulations on all 3 of these machines are about 90% parallel efficient. To put these numbers in context, consider that on 1024 processors, a million–atom simulation requires each processor to have 1000 atoms in its box. But the range of the cutoff distance in the benchmark is such that 2600 atoms from surrounding boxes are still needed at every timestep to compute forces. Thus the SD algorithm **S1** is 75–80% efficient even though two–and–a–half times as many atom positions are communicated as are updated locally by each processor.

Finally, we highlight the scalability of the different parallel algorithms in the large N limit. Table V shows the overall scaling of the computation and communication portions of the 5 algorithms. This is constructed from the scaling entries for the various steps of the algorithms in Figures 3, 4, 6, 7, and 9, using large N values when there is an option. Some coefficients are included to show contrasts between the various algorithms. The amount of memory required per processor to store atom position and force vectors is also listed in the table.

Computation in the AD algorithm **A1** scales as $N/P + N$ where the second term is for binned neighbor list construction. The coefficient on this term is small so it is usually not a significant factor. The communication scales as N, as does the memory to store all atom positions. By contrast, AD algorithm **A2** implements Newton's 3rd law so its leading computational term is cut in half. Now the communication cost is doubled and the entire force vector must be stored on each processor as well.

FD algorithms **F1** and **F2** have the same computational complexity as **A1** and **A2** respectively except the binning for neighbor list construction now scales as $N/\sqrt{P}$, again not typically a significant factor. In **F1** there are 3 expands/folds for a communication cost of $3N/\sqrt{P}$. Similarly **F2** requires 4 expands/folds. Implementing **F1** requires storing two atom position sub–vectors and one force sub–vector, all of length $N/\sqrt{P}$. **F2** requires an extra force sub–vector.

Computation in the SD algorithm **S1** scales as $N/2P$ since it implements Newton's 3rd law for interactions between atom pairs inside a processor's box. For large N problems there is an extra factor for computations performed on nearby atoms within a distance r_s of the box faces. The number of these atoms is proportional to the surface area of the box face $(N/P^{2/3})$ times r_s for each of the 6 faces. The communication in algorithm **S1** scales as the same factor as do the memory requirements for storing the nearby atoms. Additionally, $O(N/P)$ memory must be allocated for storing the atoms in a processor's box.

8 Application of the Algorithms

While the benchmark problem discussed in Sections 6 and 7 is relatively simple, the parallel algorithms described in this paper can be used in more complex MD simulations with little modificiation. For example, the following common MD calculations can be carried out in parallel within the framework of any of the

3 algorithms: on–the–fly computation of thermodynamic quantities and transport coefficients, triggering of neighbor list construction by atom movement, multiple–timescale methods [37, 50], more sophisticated time integrators, and other statistical ensembles besides the constant NVE ensemble of the benchmark, e.g. constant NPT simulations.

Virtually any form of short–range interatomic force function can be implemented within the AD or SD framework. The FD algorithm is less general in this respect. If higher–order (3–body, 4–body, etc.) interactions are included in the force model, one must insure some processor knows sufficient information to compute any given interaction. An implementation for the embedded atom method (EAM) potentials [18] used in modeling metals and metal alloys is discussed in [43] and a FD implementation of the many–body forces (angular, torsional) encountered in molecular simulations is presented in [42]. We know of no simple way to use the FD idea for the more general case of simulations with dynamically changing connectivities, such as for silicon three–body potentials. Long–range pairwise forces can be computed directly with $O(N^2)$ work in the force–matrix formalism of the AD and FD algorithms [29]. By contrast, the SD algorithm would now require long–range communication and become inefficient.

In practical terms, how does one choose the "best" parallel algorithm for a particular MD simulation? Assuming one knows the ranges of N and P the simulation will be run with, we find the following four guidelines helpful.

(A) Choose an AD algorithm only if the communication cost is expected to be negligible. In this case simplicity outweighs the inefficient communications. Typically this will only be true for small P (say $P \leq 16$ processors) or very expensive forces where computation time dominates communication time.

(B) A FD approach will be faster than AD in all other cases. Both the AD and FD algorithms scale linearly with N for fixed P. This means for a given P, the parallel efficiency of either algorithm is independent of N. Moreover, as P doubles, the communication time in the AD algorithm is unchanged, while in the FD algorithm it decreases by a factor of $\sqrt{2}$. Thus, once P is large enough that FD is noticeably faster than AD, it will remain faster as P increases, independent of N. For the benchmark problem this was the case for $P \geq 16$ processors.

(C) For a given P, the scaling of the SD algorithm is not linear with N. This is due to the fact each proccessor's box has volume $d^3 = N/P$, but it computes and communicates information in an extended volume of $(d + 2r_s)^3$, where r_s is a neighbor list cutoff distance. For small N communication and overhead costs are significant and the efficiency is poor; for large N the efficiency is asymptotically optimal (100%). Thus when compared to a FD approach, there will be some cross–over point as N increases for a given P where a SD algorithm becomes faster. In the benchmark the cross–over size was several thousands of atoms on hundreds of processors, as in Figure 10. In general, the cross–over point is a function of the complexity of the force model, force cutoff distances, and the computational and communication capabilities of a particular parallel machine. It will also be a function of P. For example, if the force cutoff distance is reduced to $r_c = 2^{1/6}\sigma$ to model a fluid with purely repulsive forces, the parallel efficiency of the FD

algorithm will decrease since the computational work per processor decreases, but the communication cost of the algorithm is independent of the cutoff length. By contrast, the efficiency of the SD approach is not as dependent on the cutoff length since both computation and communication costs decrease in this case. Thus the net effect of a shorter cutoff distance is to reduce the cross–over size at which SD becomes faster. The converse case of increasing the cutoff distance was illustrated in Figure 11.

(D) The preceding paragraph assumes the computation in the SD algorithm is perfectly load–balanced. Load–imbalance imposes an upper bound on the efficiency a SD algorithm can achieve. For example, biological simulations of proteins solvated by water may be performed in vacuum so that the atoms in the simulation fill a roughly spherical volume. If this domain is treated as a cube and split into P pieces then the sphere fills only a $\pi/6$ fraction of the cube and a 50% parallel inefficiency results. The net effect of load–imbalance is to increase the cross–over size at which a SD algorithm becomes faster than a FD approach. In practice, we have found the FD algorithm can be faster or at least quite competitive with SD algorithms for molecular simulations of up to many tens of thousands of atoms [42].

9   Conclusion

We have detailed the construction and implementation of three kinds of parallel algorithms for MD simulations with short-range forces. Each of them has advantages and disadvantages. The atom–decomposition algorithm is simplest to implement and load–balances automatically. But because it performs all–to–all communication, its communication costs begin to dominate its run time on large numbers of processors. The force–decomposition algorithm is also relatively simple, though it often requires some pre–processing to assure load–balance. It also works well independent of the physical problem's geometry. Its $O(N/\sqrt{P})$ scaling is better than that of the AD algorithm, but is not optimal for large simulations. The spatial–decomposition algorithm does exhibit optimal $O(N/P)$ scaling for large problems. However it suffers more easily from load–imbalance and is more difficult to implement efficiently.

In Section 7 we discussed the performance of the parallel algorithms on several different parallel computers. The results show that current–generation parallel machines are competitive with multi–processor Cray-class vector supercomputers for short–range MD simulations. More generally, these algorithms can be implemented on any parallel computer that allows its processors to execute code independently of each other and exchanges data between processors by standard message–passing techniques. Most of the current–generation parallel supercomputers support this mode of programming, including the nCUBE 2, Intel Paragon, TMC CM–5, and Cray T3D machines. Several features of the algorithms take advantage of the flexibility of the message–passing model for MIMD machines, including the code to build and access variable–length neighbor lists via indirect addressing, to select/pack/unpack data for messages, and to efficiently exchange variable–length data structures between sub–groups of processors as in Figures 2 and 8.

Finally, we are confident these algorithms or versions based on similar ideas will continue to be good choices for MD simulations on parallel machines of the future. Optimizing their performance for next-

generation machines will require improving their single–processor computational performance. As the individual processors used in parallel machines become faster and more complex, higher computational rates can only be achieved by writing pipelined or vectorized code, as highlighted in Section 7 for the Intel Paragon. Thus, many of the data reorganization and other optimization techniques that have been developed for MD on vector machines [24] will become important for parallel implementations as well.

10   Acknowledgments

References

[1] F. F. Abraham. Computational statistical mechanics: methodology, applications and supercomputing. *Advances in Physics*, 35:1–111, 1986.

[2] M. P. Allen and D. J. Tildesley. *Computer Simulation of Liquids*. Clarendon Press, Oxford, 1987.

[3] Attig, N. and K. Kremer, unpublished, 1993.

[4] D. J. Auerbach, W. Paul, A. F. Bakker, C. Lutz, W. E. Rudge, and F. F. Abraham. A special purpose parallel computer for molecular dynamics: Motivation, design, implementation, and application. *J. Phys. Chem.*, 91:4881–4890, 1987.

[5] A. F. Bakker, G. H. Gilmer, M. H. Grabow, and K. Thompson. A special purpose computer for molecular dynamics calculations. *J. Comp. Phys.*, 90:313–335, 1990.

[6] J. E. Barnes and P. Hut. A hierarchical $O(N \log N)$ force–calculation algorithm. *Nature*, 324:446–449, 1986.

[7] M. Barnett, L. Shuler, R. van de Geijn, S. Gupta, D. Payne, and J. Watts. Interprocessor collective communication library (Intercom). In *Proc. Scalable High Performance Computing Conference–94*, pages 357–364. IEEE Computer Society Press, 1994.

[8] M. Baskes, M. Daw, B. Dodson, and S. Foiles. Atomic–scale simulation in materials science. *Materials Research Society Bulletin*, pages 28–34, Feb 1988.

[9] D. M. Beazley, P. S. Lomdahl, N. Gronbech-Jensen, and P. Tamayo. A high performance communication and memory caching scheme for molecular dynamics on the CM–5. In *Proc. 8th International Parallel Processing Symposium*, pages 800–809. IEEE Computer Society Press, 1994.

[10] R. H. Bisseling and J. G. G. van de Vorst. Parallel LU decomposition on a transputer network. In G. A. van Zee and J. G. G. van de Vorst, editors, *Lecture Notes in Computer Science, Number 384*, pages 61–77. Springer–Verlag, 1989.

[11] B. M. Boghosian. Computational physics on the Connection Machine. *Comp. in Phys.*, Jan/Feb, 1990.

[12] L. L. Boyer and G. S. Pawley. Molecular dynamics of clusters of particles interacting with pairwise forces using a massively parallel computer. *J. Comp. Phys.*, 78:405–423, 1988.

[13] B. R. Brooks and M. Hodošček. Parallelization of CHARMM for MIMD machines. *Chemical Design Automation News*, 7:16–22, 1992.

[14] D. Brown, J. H. R. Clarke, M. Okuda, and T. Yamazaki. A domain decomposition parallelization strategy for molecular dynamics simulations on distributed memory machines. *Comp. Phys. Comm.*, 74:67–80, 1993.

[15] J. P. Brunet, A. Edelman, and J. P. Mesirov. Hypercube alborithms for direct N–body solvers for different granularities. *SIAM J. Sci. Stat. Comput.*, 14(5):1143–1158, September 1993.

[16] J. P. Brunet, J. P. Mesirov, and A. Edelman. An optimal hypercube direct N–body solver on the Connection Machine. In *Proc. Supercomputing '90*, pages 748–752. IEEE Computer Society Press, 1990.

[17] T. W. Clark, J. A. McCammon, and L. R. Scott. Parallel molecular dynamics. In *Proc. 5th SIAM Conference on Parallel Processing for Scientific Computing*, pages 338–344. SIAM, 1992.

[18] M. S. Daw and M. I. Baskes. Embedded–atom method: Derivation and application to impurities, surfaces, and other defects in metals. *Phys. Rev. B*, 29:6443–6453, 1984.

[19] H. Q. Ding, N. Karasawa, and W. A. Goddard III. Atomic level simulations on a million particles: The cell multipole method for Coulomb and London interactions. *J. Chem. Phys.*, 97:4309, 1992.

[20] K. Esselink, B. Smit, and P. A. J. Hilbers. Efficient parallel implementation of molecular dynamics on a toroidal network: I. Parallelizing strategy. *J. Comp. Phys.*, 106:101–107, 1993.

[21] D. Fincham. Parallel computers and molecular simulation. *Molec. Sim.*, 1:1–45, 1987.

[22] G. C. Fox, M. A. Johnson, G. A. Lyzenga, S. W. Otto, J. K. Salmon, and D. W. Walker. *Solving Problems on Concurrent Processors: Volume 1*. Prentice Hall, Englewood Cliffs, NJ, 1988.

[23] L. Greengard and V. Rokhlin. A fast algorithm for particle simulations. *J. Comp. Phys.*, 73:325–348, 1987.

[24] G. S. Grest, B. Dünweg, and K. Kremer. Vectorized link cell Fortran code for molecular dynamics simulations for a large number of particles. *Comp. Phys. Comm.*, 55:269–285, 1989.

[25] S. Gupta. Computing aspects of molecular dynamics simulations. *Comp. Phys. Comm.*, 70:243–270, 1992.

[26] H. Heller, H. Grubmuller, and K. Schulten. Molecular dynamics simulation on a parallel computer. *Molec. Sim.*, 5:133–165, 1990.

[27] B. Hendrickson and R. Leland. An improved spectral graph partitioning algorithm for mapping parallel computations. *SIAM J. Sci. Stat. Comput.*, 1994. To appear.

[28] B. Hendrickson and D. Womble. The torus–wrap mapping for dense matrix calculations on massively parallel computers. *SIAM J. Sci. Stat. Comput.*, 15:1201, 1994.

[29] B. A. Hendrickson and S. J. Plimpton. Parallel many–body simulations without all–to–all communication. *J. Par. and Dist. Comp.*, 27:15, 1995.

[30] D. M. Heyes and W. Smith. *Inf. Q. Computer Simulation Condensed Phases (Daresbury Laboratory)*, 28:63, 1988.

[31] R. W. Hockney and J. W. Eastwood. *Computer Simulation Using Particles*. Adam Hilger, New York, NY, 1988.

[32] R. W. Hockney, S. P. Goel, and J. W. Eastwood. Quiet high–resolution computer models of a plasma. *J. Comp. Phys.*, 14:148–158, 1974.

[33] J. G. Lewis and R. A. van de Geijn. Distributed memory matrix–vector multiplication and conjugate gradient algorithms. In *Proc. Supercomputing '93*, pages 484–492. IEEE Computer Society Press, 1993.

[34] Lomdahl, P. S. at Los Alamos National Labs, personal communication, 1994.

[35] A. B. Maccabe, K. S. McCurley, R. Riesen, and S. R. Wheat. SUNMOS for the Intel Paragon: A brief user's guide. In *Proceedings of the Intel Supercomputer User's Group. 1994 Annual North America Users' Conference.*, 1994.

[36] J. J. Morales and M. J. Nuevo. Comparison of link–cell and neighbourhood tables on a range of computers. *Comp. Phys. Comm.*, 69:223–228, 1992.

[37] A. Nakano, P. Vashishta, and R. K. Kalia. Parallel multiple–time–step molecular dynamics with three–body interaction. *Comp. Phys. Comm.*, 77:303–312, 1993.

[38] S. S. Patnaik, R. Pachter, S. J. Plimpton, and W. W. Adams. Molecular dynamics simulation of a cyclic siloxane based liquid crystalline material. In *Electrical, Optical, and Magnetic Properties of Organic Solid State Materials*, volume 328, pages 711–716. Materials Research Society Symposium Proc., Fall 1993.

[39] M. R. S. Pinches, D. J. Tildesley, and W. Smith. Large–scale molecular dynamics on parallel computers using the link–cell algorithm. *Molec. Sim.*, 6:51–87, 1991.

[40] S. J. Plimpton. Molecular dynamics simulations of short–range force systems on 1024–node hypercubes. In *Proc. 5th Distributed Memory Computing Conference*, pages 478–483. IEEE Computer Society Press, 1990.

[41] S. J. Plimpton. Scalable parallel molecular dynamics on MIMD supercomputers. In *Proc. Scalable High Performance Computing Conference–92*, pages 246–251. IEEE Computer Society Press, 1992.

[42] S. J. Plimpton and B. A. Hendrickson. A new parallel method for molecular dynamics simulation of macromolecular systems. Technical Report SAND94–1862, Sandia National Laboratories, Albuquerque, NM, 1994. Submitted for publication.

[43] S. J. Plimpton and B. A. Hendrickson. Parallel molecular dynamics with the embedded atom method. In *Materials Theory and Modeling*, volume 291, pages 37–42. Materials Research Society Symposium Proc., Fall 1992.

[44] S. J. Plimpton and E. D. Wolf. Effect of interatomic potential on simulated grain–boundary and bulk diffusion: A molecular dynamics study. *Phys. Rev. B*, 41:2712–2721, 1990.

[45] D. C. Rapaport. Large–scale molecular dynamics simulation using vector and parallel computers. *Comput. Phys. Rep.*, 9:1–53, 1988.

[46] D. C. Rapaport. Multi–million particle molecular dynamics: II. Design considerations for distributed processing. *Comp. Phys. Comm.*, 62:217–228, 1991.

[47] M. Schöen. Structure of a simple molecular dynamics Fortran program optimized for Cray vector processing computers. *Comp. Phys. Comm.*, 52:175–185, 1989.

[48] H. Schreiber, O. Steinhauser, and P. Schuster. Parallel molecular dynamics of biomolecules. *Parallel Computing*, 18:557–573, 1992.

[49] W. Smith. Molecular dynamics on hypercube parallel computers. *Comp. Phys. Comm.*, 62:229–248, 1991.

[50] W. B. Street, D. J. Tildesley, and G. Saville. Multiple timestep methods in molecular dynamics. *Mol. Phys.*, 35:639–48, 1978.

[51] P. Tamayo and R. Giles. A parallel scalable approach to short–range molecular dynamics on the CM–5. In *Proc. Scalable High Performance Computing Conference–92*, pages 240–245. IEEE Computer Society Press, 1992.

[52] P. Tamayo, J. P. Mesirov, and B. M. Boghosian. Parallel approaches to short–range molecular dynamics simulations. In *Proc. Supercomputing '91*, pages 462–470. IEEE Computer Society Press, 1991.

[53] P. A. Taylor, J. S. Nelson, and B. W. Dodson. Adhesion between atomically flat metallic surfaces. *Phys. Rev. B*, 44:5834–5841, 1991.

[54] R. van de Geijn. Efficient global combine operations. In *Proc. 6th Distributed Memory Computing Conference*, pages 291–294. IEEE Computer Society Press, 1991.

[55] L. Verlet. Computer experiments on classical fluids: I. Thermodynamical properties of Lennard–Jones molecules. *Phys. Rev.*, 159:98–103, 1967.

[56] M. S. Warren and J. K. Salmon. A parallel treecode for gravitational N–body simulations with up to 20 million particles. *Bulletin of the American Astronomical Society*, 23:1345, 1991.

[57] A. Windemuth and K. Schulten. Molecular dynamics simulation on the Connection Machine. *Molec. Sim.*, 5:353–361, 1991.

Figure 1: The division of the force matrix among 8 processors in the atom–decomposition algorithm. Processor 2 is assigned N/P rows of the matrix and the corresponding x_2 piece of the position vector. In addition, it must know the entire position vector x (shown spanning the columns) to compute the matrix elements in F_2.

Figure 2: *Expand* and *fold* operations among 8 processors, each of which requires 3 steps. (a) In the expand, processor 2 receives successively longer shaded sub−vectors from processors 3, 0, and 6. (b) In the fold, processor 2 receives successively shorter shaded sub−vectors from processors 6, 0, and 3.

(1) **Construct** neighbor lists of non–zero interactions in F_z	
$\quad$ ($D < 4r_s$) All pairs	$\frac{N^2}{P}$
$\quad$ ($D \geq 4r_s$) Binning	$\frac{N}{P} + N$
(2) **Compute** elements of F_z, summing results into f_z	$\frac{N}{P}$
(4) **Update** atom positions in x_z using f_z	$\frac{N}{P}$
(5) **Expand** x_z among all processors, result is x	N

Figure 3: Single timestep of atom–decomposition algorithm **A1** for processor P_z.

(1) **Construct** neighbor lists of non–zero interactions in G_z	
$\quad$ ($D < 4r_s$) All pairs	$\frac{N^2}{2P}$
$\quad$ ($D \geq 4r_s$) Binning	$\frac{N}{2P} + N$
(2) **Compute** elements of G_z,	
$\quad$ doubly summing results into local copy of f	$\frac{N}{2P}$
(3) **Fold** f among all processors, result is f_z	N
(4) **Update** atom positions in x_z using f_z	$\frac{N}{P}$
(5) **Expand** x_z among all processors, result is x	N

Figure 4: Single timestep of atom–decomposition algorithm **A2** for processor P_z, which takes advantage of Newton's 3rd law.

Figure 5: The division of the permuted force matrix F' among 16 processors in the force–decomposition algorithm. Processor P_6 is assigned a sub–block F'_6 of size $N/\sqrt{P}$ by $N/\sqrt{P}$. To compute its matrix elements it must know the corresponding $N/\sqrt{P}$-length pieces x_α and x'_β of the position vector x and permuted position vector x'.

(1) **Construct** neighbor lists of non–zero interactions in F'_z	
$(D < 4r_s)$ All pairs	$\frac{N^2}{P}$
$(D \geq 4r_s)$ Binning	$\frac{N}{P} + \frac{N}{\sqrt{P}}$
(2) **Compute** elements of F'_z, storing results in f_α	$\frac{N}{P}$
(3) **Fold** f_α within row α, result is f_z	$\frac{N}{\sqrt{P}}$
(4) **Update** atom positions in x_z using f_z	$\frac{N}{P}$
(5a) **Expand** x_z within row α, result is x_α	$\frac{N}{\sqrt{P}}$
(5b) **Expand** x_z within column β, result is x'_β	$\frac{N}{\sqrt{P}}$

Figure 6: Single timestep of force–decomposition algorithm **F1** for processor P_z.

(1) **Construct** neighbor lists of non–zero interactions in G'_z	
$(D < 4r_s)$ All pairs	$\frac{N^2}{2P}$
$(D \geq 4r_s)$ Binning	$\frac{N}{2P} + \frac{N}{\sqrt{P}}$
(2) **Compute** elements of G'_z, storing results in f_α and f'_β	$\frac{N}{2P}$
(3a) **Fold** f'_β within column β, result is f'_z	$\frac{N}{\sqrt{P}}$
(3b) **Fold** f_α within row α, result is f_z	$\frac{N}{\sqrt{P}}$
(3c) **Subtract** f'_z from f_z, result is total f_z	$\frac{N}{P}$
(4) **Update** atom positions in x_z using f_z	$\frac{N}{P}$
(5a) **Expand** x_z within row α, result is x_α	$\frac{N}{\sqrt{P}}$
(5b) **Expand** x_z within column β, result is x'_β	$\frac{N}{\sqrt{P}}$

Figure 7: Single timestep of force–decomposition algorithm **F2** for processor P_z, which takes advantage of Newton's 3rd law.

Figure 8: Method by which a processor acquires nearby atom positions in the spatial–decomposition algorithm. In 6 data exchanges all atom positions in adjacent boxes in the (a) east/west, (b) north/south, and (c) up/down directions can be communicated.

(1a) **Move** necessary atoms to new boxes	Δ
(1b) **Make** lists of all atoms that will need to be exchanged	Δ
(1c) **Construct** neighbor lists of interaction pairs in box z	
$(d < 2r_s)$ All pairs	$\frac{N}{P}(\frac{N}{2P} + \Delta)$
$(d \geq 2r_s)$ Binning	$\frac{N}{2P} + \Delta$
(2) **Compute** forces on atoms in box z, doubly storing results in f_z	$\frac{N}{2P} + \Delta$
(4) **Update** atom positions x_z in box z using f_z	$\frac{N}{P}$
(5) **Exchange** atom positions across box boundaries	
with neighboring processors	$\frac{N}{P}(1 + 2r_s/d)^3$
$(d < r_s)$ Send N/P positions to many neighbors	$r_s{}^3$
$(d \approx r_s)$ Send N/P positions to nearest neighbors	$\frac{N}{P}$
$(d > r_s)$ Send positions near box surface to nearest neighbors	$(\frac{N}{P})^{2/3}$

Figure 9: Single timestep of spatial–decomposition algorithm **S1** for processor P_z.

Table IV: CPU seconds/timestep for optimized versions of the spatial–decomposition algorithm **S1** on the Intel Paragon for the benchmark simulation. The first two columns are for the Fortran version of the code run in single– and dual–processor mode. The second two columns are timings with an assembler version of the force–computation subroutine, again for single– and dual–processor mode.
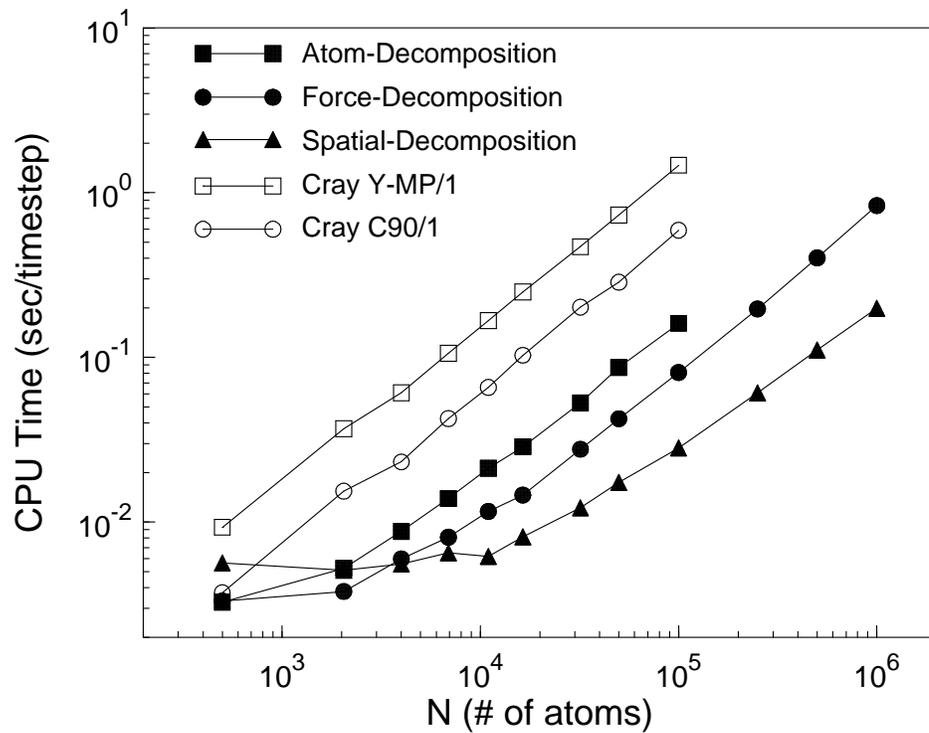
Figure 10: CPU timings (seconds/timestep) for the three parallel algorithms on 1024 processors of the Intel Paragon for different problem sizes. Single–processor Cray Y–MP and C90 timings are also given for comparison.
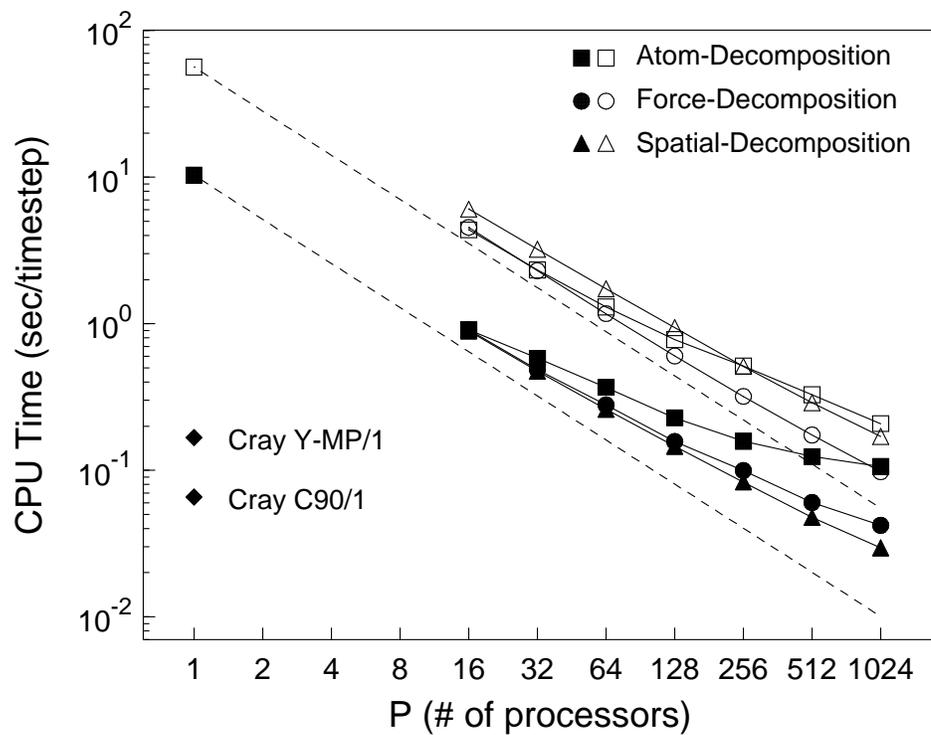
Figure 11: CPU timings (seconds/timestep) for the three parallel algorithms on the nCUBE 2 for different numbers of processors on the benchmark simulation with $N = 10976$ atoms for two different force cutoff lengths. Single–processor Cray Y–MP and C90 timings are shown for comparison.

Table V: Scaling properties of all 5 parallel algorithms as a function of problem size N and number of processors P. Run time scaling for the computation and communication portions of the algorithms as well as their per–processor memory requirements are listed.